

HOW DO GALAXIES BECOME RED AND DEAD?

Ángela Abad Martín

Supervisors: Pablo Corcho-Caballero and Violeta González Pérez

Acknowledgements: Yago Ascasibar Sequeiros

May 2023, Tutorized Bachelor Thesis

Summary

Determining the star formation history of galaxies in order to describe their evolution is a complex process, considered a challenge within the scientific community. The following project is based on a previous spectroscopic study that classifies galaxies in an “Aging Diagram” based on whether they evolve gradually (ageing) or whether they suffer a violent episode that truncates their star formation (quenching). As an alternative, photometric techniques are then used to carry out this classification. It starts from a sample of around 150,000 galaxies in the Local Universe belonging to the GAMA spectroscopic project, whose data are analyzed to create color-color diagrams that allow quenched galaxies to be excluded from the rest. As a result, through the combination of the bands $u - g$ compared to $g - K$, it is possible to discern between two evolutionary paths. This opens up the possibility of studying the different populations of galaxies based on their evolutionary state using photometric data.

Index

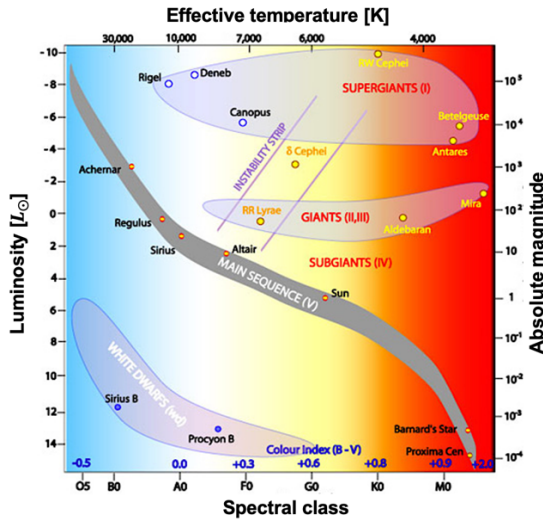
1.	Introduction	1
1.1.	Evolution of galaxies	1
1.2.	Previous studies	2
1.2.1.	Equivalent width of H α line and Balmer jump at 4000Å	2
1.2.2.	Demarcation lines for galaxy classification	4
2.	Methodology.....	4
2.1.	Spectroscopic analysis: Ageing Diagram	5
2.2.	Photometric analysis	6
2.2.1.	Advantages over spectroscopy.....	6
2.2.2.	Theoretical foundations	7
2.2.3.	Analysis for the representation of color-color diagrams.....	8
3.	Result.....	12
4.	Discussion.....	14
5.	Conclusions	16

1. Introduction

1.1. Evolution of galaxies

The study of the evolutionary development of galaxies has always been a matter of great interest. A galaxy begins its star formation from the collapse of molecular clouds in the interstellar medium ([Star formation, sf](#)), giving rise to a spectrum of different stellar masses that generally encompasses the entire main sequence (MS) ([F. Lopez, 2019](#)) (see *Figure 1*), from more massive, hot and bright stars (blue) to less massive, cold and weaker luminosities (red). Likewise, the blue stars of the MS (despite not necessarily being the majority type in the population) dominate the light of the galaxy by their luminosity, giving it that same bluish tone.

Figure 1. HR Diagram (Hertzsprung Russell): shows the different stellar evolutionary phases ([Ashtray, 2011](#)).



On the other hand, star formation in galaxies is affected by multiple physical processes that, in general, cause fewer and fewer stars to be created ([Kormendy & Kennicutt Jr, July 16, 2004](#)). This causes the galaxy to transition in color from blue (with a predominantly young population) to red (with older and/or inactive stars) due to the aging of these stars and the lack of their replacement by new ones.

Initially, a paradigm was established that is still valid based on the process of evolution of galaxies from blue to red through what is known as *quenching* (evolutionary truncation) ([Peng, Maiolino, & Cochrane, May 14, 2015](#)). This process consists of the reduction of the star formation rate (SFR) of the galaxy in a violent way due to both internal effects (i.e. the action of an active galactic nuclei or a supernova explosion) and

from the environment (i.e. ram pressure, tidal effects due to the cluster potential, starvation...) (Correse, Catinella, & Smith, 2021).

Instead, recent studies suggest a model in which red galaxies do not necessarily arise from a process of *quenching*, but may have evolved from blue by *ageing* (Corcho-Caballero et al. January 13, 2023). This is a gradual development of the galaxy, maintaining a SFR that gradually decreases without violent changes. In this way, a new paradigm of evolution is proposed through two types of sequences: *ageing* and *quenching*. This turns out to be the fundamental model with which we work during the study.

1.2. Previous studies

The main objective of the project is based on the identification of galaxies based on their evolutionary sequence using photometry. This is done based on previous studies (Corcho-Caballero et al., July 29, 2021; Corcho-Caballero et al., January 13, 2023) in which, through computational models and spectroscopic techniques, a population discrimination scheme called Ageing Diagram (AD) is determined. This is characterized by parameters that are sensitive to different stellar populations and time scales, such as the equivalent width (Equivalent width, sf) from the H_{α} line and the Balmer jump (Balmer Jump, 2021) at 4000Å. In this way, phenomenological demarcation lines are established that introduce the criterion of discrimination between the two evolutionary paths.

1.2.1. Equivalent width of H_{α} line and Balmer jump at 4000Å

$EW(H_{\alpha})$ is the equivalent width of the H_{α} line, defined as the ratio between the flux in the spectrum region around $\lambda_{H_{\alpha}} \sim 6563\text{\AA}$ ($F(\lambda)$) and the flux density of the continuous spectrum of the object (F_c), (Corcho-Caballero et al., January 13, 2023),

$$EW(H_{\alpha}) [\text{\AA}] = \int_{6550\text{\AA}}^{6575\text{\AA}} \left(\frac{F(\lambda)}{F_c} - 1 \right) d\lambda \quad (1)$$

The spectrum of stars is characterized by a continuum that generally presents absorption lines (Martinez Martinez, 2018). Additionally, when there is presence of gas in the interstellar medium and it is ionized, emission lines also appear in the spectra. In the case of hydrogen, it is completely ionized around $1,5 \cdot 10^4 K$ (Hydrogen-H, sf; Saha ionization equilibrium equation, sf).

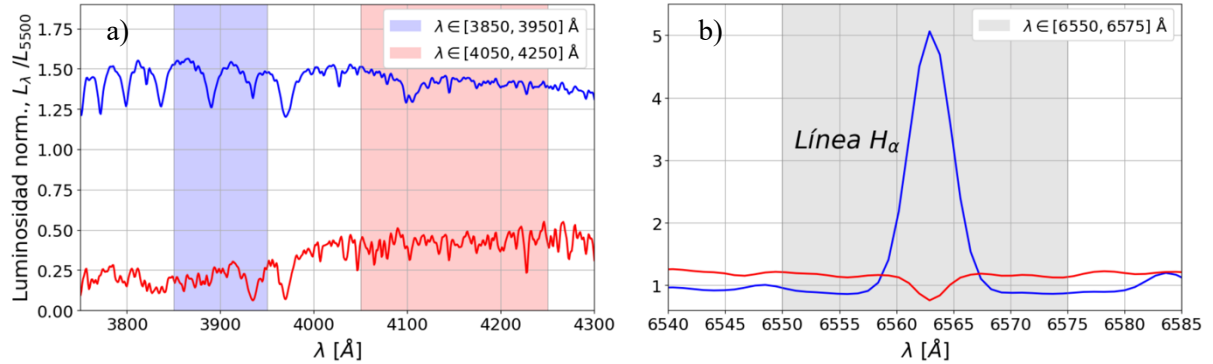
O and B type stars, as they exceed this temperature (see Figure 1), ionize the hydrogen in the interstellar medium, presenting emission lines of the gas that predominate over the absorption lines of their spectrum. On the other hand, type A stars (see Figure 1), have a temperature below the ionization temperature, an optimal case for the absorption of the line. Therefore, for galaxies with a predominance of O and B stars (blue) intense emission lines are recorded ($EW(H_\alpha) > 0$) while for galaxies with an absence of this type of stars absorption lines are detected ($EW(H_\alpha) < 0$). Therefore, this parameter is associated with short time scales ($\sim 10 - 30$ Myr), given by the average lifetime of the O and B type stars that characterize the emission line (see Figure 2b).

$D_n(4000)$, on the other hand, represents the jump in the spectral distribution of the galaxy around 4000Å (close to optical). It is defined as the ratio of average flux densities between the near-visible range ($\langle F_\lambda \rangle_{(4050-4250)\text{\AA}}$) and near ultraviolet ($\langle F_\lambda \rangle_{(3850-3950)\text{\AA}}$). In other words, it is the value of the slope between both bands, giving the following result (Corcho-Caballero et al., January 13, 2023)

$$D_n(4000)[\text{adim.}] = \frac{\langle F_\lambda \rangle_{(4050-4250)\text{\AA}}}{\langle F_\lambda \rangle_{(3850-3950)\text{\AA}}} \quad (2)$$

Similarly to the previous case, $D_n(4000)$ provides information about the stellar characteristics of galaxies: if there is a predominance of young ionizing stars (type O and B) or of high temperatures (type A), the Balmer jump turns out to be more discrete and even imperceptible (low $D_n(4000)$) since the flux density in the ultraviolet band exceeds that of the visible ($\langle F_\lambda \rangle_{(3850-3950)\text{\AA}} > \langle F_\lambda \rangle_{(4050-4250)\text{\AA}}$); on the other hand, if stellar populations of lower temperatures (type F and onwards) and/or longer-lived predominate, greater radiation is produced in the visible region than in the ultraviolet ($\langle F_\lambda \rangle_{(3850-3950)\text{\AA}} < \langle F_\lambda \rangle_{(4050-4250)\text{\AA}}$, high $D_n(4000)$). As a consequence, this parameter is associated with long time scales ($\sim 1\text{Gyr} = 10^9$ yr), the average life span of type A stars that delimit the two behaviors (see Figure 2a).

Figure 2. Comparison of the spectrum of two galaxies: with young stellar population (blue) and old one (red).
a) Balmer jump at 4000 Å. b) Equivalent width of the H_α line.



1.2.2. Demarcation lines for galaxy classification

Developing a combination of galaxy formation simulations (ILLUSTRIS TNG) ([The IllustrisTNG project, sf](#)) and astronomical observations with spectroscopic techniques from projects such as CALIFA (Calar Alto Legacy Integral Field Area) ([CALIPH, sf](#)) and MaNGA (Mapping Nearby Galaxies at APO)([MaNGA, sf](#)), previous studies define the regions for each population by means of two phenomenological demarcation lines given by the following expression ([Corcho-Caballero et al., January 13, 2023](#))

$$EW(D_n(4000)) = k \cdot 10^{\alpha \cdot D_n(4000)} + EW_{\infty}$$

$$\text{Ageing sequence line: } k = 250 \text{ Å}, \alpha = -1,2 \text{ [adim.], } EW_{\infty} = -4,3 \text{ Å} \quad (3)$$

$$\text{Quenching sequence line: } k = -12 \text{ Å}, \alpha = -0,5 \text{ [adim.], } EW_{\infty} = 1,8 \text{ Å}$$

where k and α refer to parameterization constants and EW_{∞} is the equivalent width of the H_α absorption line given by populations of veteran stars. These lines allow the AD plane to be theoretically divided into four regions, a process that is demonstrated below (see Figure 3).

2. Methodology

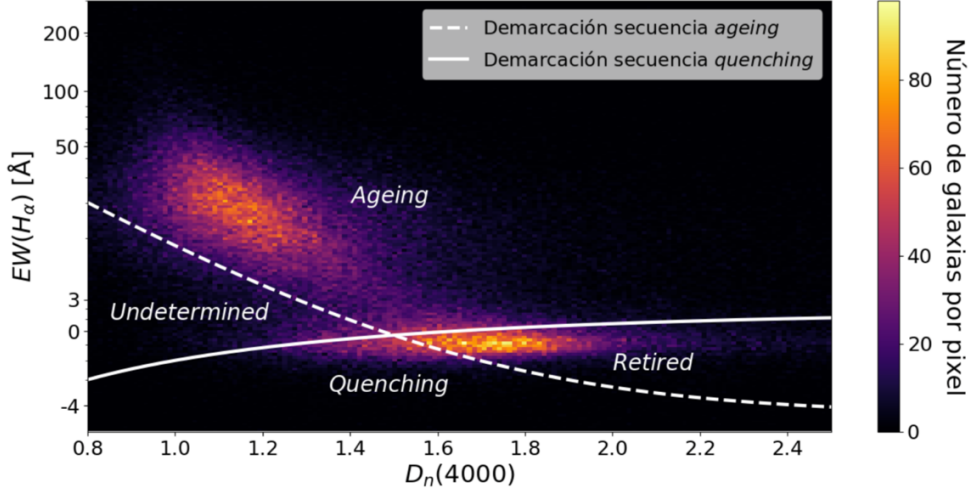
Once the sequences by which galaxies are expected to evolve during their lifetime have been defined, an alternative for the identification of quenching galaxies through photometry is proposed below.

It is based on a sample of around 150,000 galaxies of the Local Universe belonging to the GAMA (Galaxy And Mass Assembly) project ([Project overview, sf](#)). This brings together data from the AAOmega team at the Anglo-Australian Telescope (AAT), Australia. Initially, by means of a spectroscopic analysis based on previous

studies (see section 1.2.), the AD of the sample is represented, tracing the distinction of populations from the lines proposed in equation (3). Subsequently, a multifrequency analysis is performed through the manipulation of the galaxy data to “recreate” a variant of the spectroscopic AD with photometry in the form of color-color diagrams.

2.1. Spectroscopic analysis: Ageing Diagram

Figure 3. Ageing Diagram.



Representing the parameters $EW(H_\alpha)$ and $D_n(4000)$ (Spectroscopic data (information by private communication)) and introducing the demarcation lines according to equation (3), the corresponding AD is plotted for the sample of galaxies used, characterizing four different populations.

Ageing galaxies show very low $D_n(4000)$ indices and high values of $EW(H_\alpha)$ due to the predominant presence of O and B type stars ionizing the interstellar medium.

On the other hand, there is the case of slightly bluish galaxies associated with low $D_n(4000)$ indices (indicating the presence of populations of young stars on long time scales (type A)), but which are also characterized by reduced $EW(H_\alpha)$ values (implying the scarcity of ionizing stellar population). These are quenching galaxies, whose star formation is interrupted, drastically reducing the population of O and B stars by supernova explosions, causing type A stars to dominate.

If, on the other hand, galaxies with high $D_n(4000)$ indices are considered and low $EW(H_\alpha)$ values, we speak of retired galaxies, characterized by being red and presenting a very small or practically null SFR.

Finally, undetermined galaxies are those located between the aging and quenching stages and whose properties and evolutionary characteristics remain unknown to this day, as they could well be galaxies undergoing truncation (quenching) or rejuvenation (through a burst of star formation). For this reason, as they are complex to classify observationally, they are not taken into account during the study.

In conclusion, the AD diagram makes a distinction between ageing and quenched galaxies, which can evolve based on their properties through the ageing sequence (above the ageing demarcation line) and quenching (below the quenching demarcation line) respectively, both ending their evolutionary process in the retired galaxy region (point of intersection). Once the galaxy was found in this region, it would be impossible to distinguish through which sequence it had evolved. It should be noted that the *ageing* mechanism is intrinsic to all galaxies because it is a natural, progressive and aging process just as it occurs with the rest of the biological processes in nature. Only the *quenching* would affect a small fraction of galaxies ([Corcho-Caballero et al., January 13, 2023](#)).

2.2. Photometric analysis

2.2.1. Advantages over spectroscopy

Spectroscopy techniques ([Spectroscopy in Astronomy, n.d.; Spectroscopy in astronomy, n.d.](#)), despite allowing precise measurement of galaxy spectra and therefore the parameters mentioned above, they present several drawbacks to be taken into consideration such as the long exposure times required and the aperture effects. ([Maragkoudaki, Zezas, Ashby, & Willner, May 19, 2014](#)).

The first of all makes this a less efficient and more laborious (expensive) technique, which implies the measurement of groups of no more than hundreds of galaxies at a time. The second drawback arises from the measurement method itself; it is quite common for regions of the galaxy to be left outside the material that collects the spectra and, therefore, the data obtained usually represent only the central region of the galaxy, generally giving redder results because that is where the veteran stars tend to predominate. ([Galactic bulge, sf](#)).

Instead, the photometry technique ([Photometry, sf; Galadi Enriquez, 2022; Photometry](#)) allows the apparent brightness of celestial bodies to be determined by

measuring the energy flow obtained in different bands. This technique collects photons in different ranges of the spectrum to characterize it more roughly, thus allowing working with a larger number of galaxies (greater data statistics) and using a shorter exposure time (faster procedure). As a result, it provides a spectrum with less information than that obtained with spectroscopy, but allows for a more accessible qualitative analysis.

2.2.2. Theoretical foundations

Photometry generates low-resolution spectra of astronomical bodies. To do this, it uses filters that allow light from galaxies to pass through them in a certain spectral range (photometric band) ([Photometric system, sf](#); [Richer, 2022](#)), prohibiting photons of frequencies outside this range can penetrate.

On the other hand, the brightness of astronomical objects is quantified from the apparent magnitude([Apparent magnitude, sf](#)), which gives information about the light received from said body. It is given by the following expression,

$$m_{banda} = -2,5 \cdot \log_{10} \left(\frac{F_{banda}}{\mathcal{F}} \right) \quad (4)$$

where m_{banda} is the apparent magnitude of the object in a given photometric band, F_{banda} is the flux measured in that band and $\mathcal{F} = 3631 \text{ Jy}$ is the reference spectral flux density at $m = 0$ ($1 \text{ Jy} = 10^{-26} \text{ W}/(\text{m}^2 \cdot \text{Hz})$) ([Jansky \(unit\), sf](#)).

For the photometric study in question, the objective is to determine combinations of color indices ([Richmond, sf](#)) from the fluxes of the different galaxies in different photometric bands (multifrequency analysis). In this way, the color can be defined as a ratio of magnitudes, one of them being bluer and the other redder within the chosen combination:

$$m_{azul} - m_{rojo} = -2,5 \cdot \log_{10} \left(\frac{F_{azul}}{F_{rojo}} \right) \quad (5)$$

Thus, m_{azul} and F_{azul} are the magnitude and flux of the object in the blue band of the chosen pair and m_{rojo} and F_{rojo} are the magnitude and flux in the red band. Also, from relation (5) it is worth noting that during the calculation of any colour the reference parameters cancel each other out, leaving only the value of the flux measured in each band.

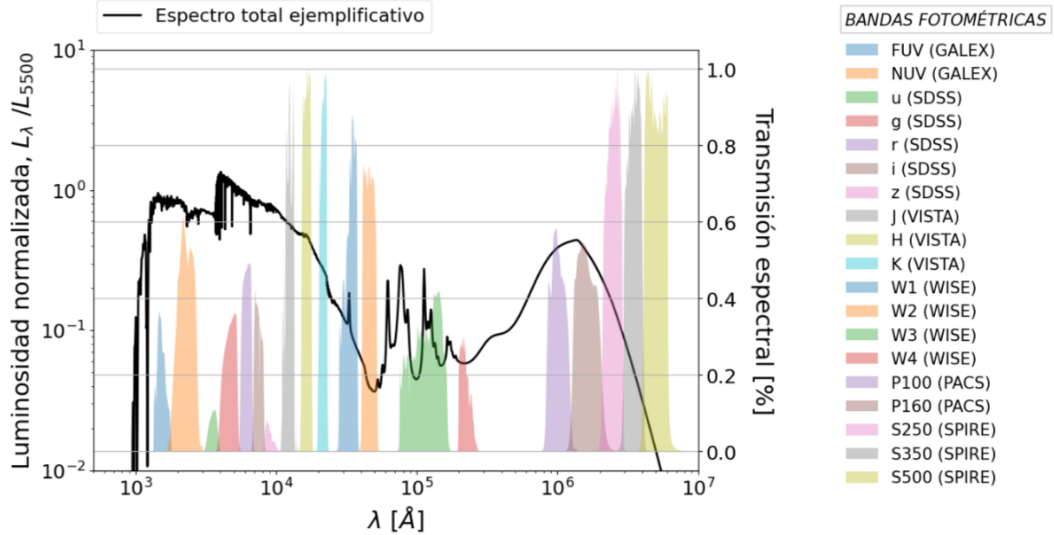
By combining different colors, a wide variety of pairs are obtained with which color-color diagrams are represented. ([Color-color diagram, sf](#)), a fundamental tool on which the evolutionary distinction analysis of this project is based.

2.2.3. Analysis for the representation of color-color diagrams

Next, the LAMBDA catalogue is used ([Wright, Robotham, & Bourne, April 12, 2016](#)) (available at GAMA), a database that compiles information on the galaxy sample in a multi-frequency range of 21 photometric bands. It covers the electromagnetic spectrum from the far ultraviolet to the far infrared and arises from a collaboration with the following telescopes and surveys:

- GALEX (GALaxy Evolution eXplorer): satellite that provides the region between the far and near ultraviolet (*FUV* and *NUV* bands).
- SDSS (Sloan Digital Sky Survey): astronomical survey project delimited in the optical region (*u, g, r, i, z* bands).
- VISTA (Visible and Infrared Survey Telescope for Astronomy): telescope belonging to the VIKING (Vista Kilo-degree Infrared Galaxy survey) survey and which characterizes the near-infrared region (*X, Y, J, H, K* bands).
- WISE (Wide-Field Infrared Survey Explorer): satellite that delimits images in the mid-infrared spectrum (*W1, W2, W3, W4* bands).
- PACS (Physics and Astronomy Classification Scheme) and SPIRE (*Spectral and Photometric Imaging Receiver*): instruments of the Herchel Space Observatory for characterizing images in the far infrared, from $100\mu m$ to $500\mu m$ (*P100, P160, S250, S350 y S500* bands).

Figure 4. Exemplification of the range covered by the photometric bands. The response function associated with the X and Y bands could not be found, so they are not represented (although they are used).



The bands (see figure 4) of the ultraviolet characterize the area of the spectrum dominated by the formation of young stars while the region from the optical to the band $W2$ defines the bulk of the stellar mass (contributing both young and old stars). On the other hand, the distant WISE bands ($W3$ and $W4$) represent the warm dust of the interstellar medium and, finally, the area delimited by the bands of the PACS and SPIRE instruments represent the thermal emission of the cold dust.

It is relevant to mention that the LAMBDAR catalogue reduces the sample from 150,000 galaxies to about 100,000 due to a lack of completeness in its archival data.

Signal-to-noise filter

Initially, color-color combinations were developed for the entire range of available bands. However, after noticing that no differentiation was observed between the populations applying the same criterion of distinction as in the AD, a signal-to-noise ratio (SNR) analysis was continued (Noise, signal and SNR in amateur astrophotography, 2016).

Every data collection presents an associated error. When handling samples with sufficient statistics (~ 100.000 galaxies) it is necessary to perform an analysis based on the noise present in the measured data, which sometimes only blurs the results instead of providing clarity. Thus, this correction consists of eliminating those values that do not provide relevant information to the study.

The SNR parameter is defined as the ratio of the galaxy fluxes in each of their photometric bands (F_{banda}) and their corresponding associated errors (ΔF_{banda}),

$$SNR = \frac{F_{banda}}{\Delta F_{banda}} \quad (6)$$

On the one hand, from relation (4) it is determined that the apparent magnitude is proportional to the flux such that $m_{banda} = -2,5 \cdot \log_{10}(F_{banda}) + C$ (with $C \equiv$ constant). By propagation of errors of the magnitude with respect to said flow it is determined that:

$$\Delta m_{banda} = \left| \frac{\partial m_{banda}}{\partial F_{banda}} \right| \Delta F_{banda} \Rightarrow \Delta m_{banda} = \frac{2,5}{SNR \cdot \ln(10)} \quad (7)$$

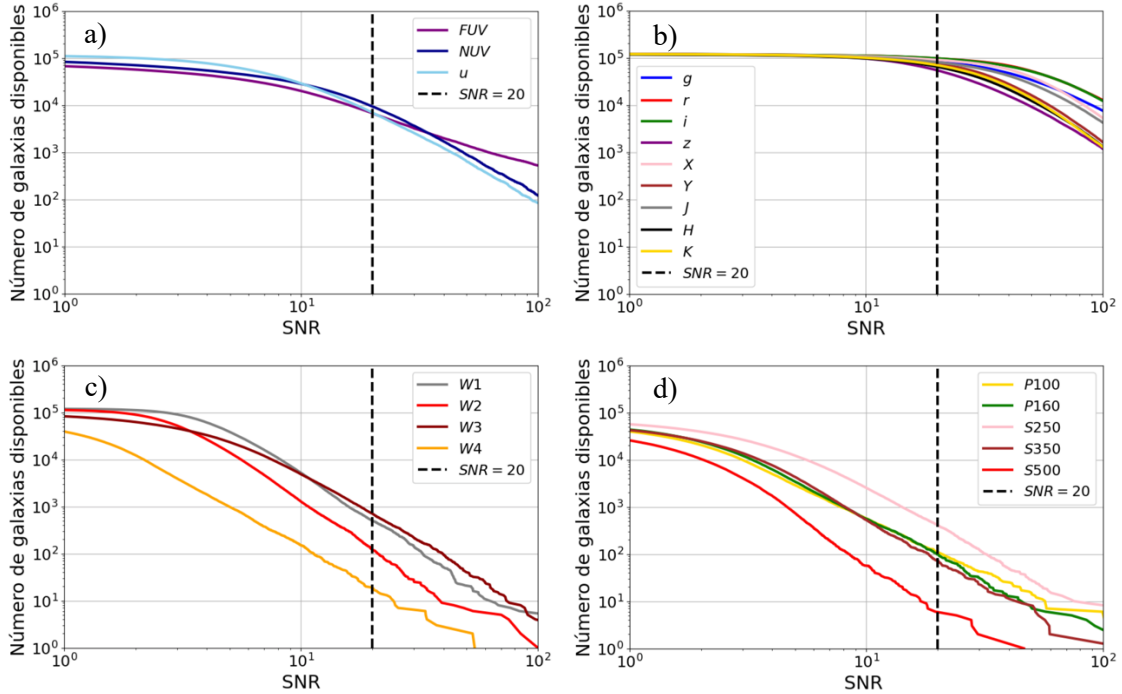
where the relation (6) has been used and from which it is observed that the error in the apparent magnitude for a given band is proportional to the inverse of the signal-noise. Through an experimental iterative process it is determined that the difference necessary between two magnitudes (color) to work with such precision that populations can be distinguished is

$$\Delta(m_{azul} - m_{rojo}) = \sqrt{\Delta m_{azul}^2 + \Delta m_{rojo}^2} \sim [0,05 - 0,1] \quad (8)$$

Assuming that the errors for different bands are approximately equal to each other and are given by the relation (7), the need to introduce a signal-to-noise limit of $SNR = 20$ value is verified.

Once this filter is introduced, its effect is checked on the photometric bands, representing the number of galaxies for each one as a function of the chosen limit (see figure 5). Figures 5c and 5d show that for $SNR = 20$, the number of galaxies available and associated with rigorous data is between 10 and 1,000 for these bands (mid-far infrared). These are considerably lower values compared to the starting 100.000 galaxies. These results, therefore, suggest that the photometric data in this range barely meet the imposed conditions, giving a sample of galaxies with hardly any statistics, which makes population analysis difficult. For this reason, these bands are ignored in the study.

Figure 5. Number of galaxies versus signal-to-noise ratio ($SNR = 20$) for each photometric band.
a) Ultraviolet. b) Optical -- Near-infrared. c) WISE (mid-infrared). d) Far-infrared.



On the other hand, Figure 5b represents the photometric range with the best signal-to-noise ratio, maintaining, to a good approximation, the complete sample of galaxies. This is why we work mainly with bands from the optical to the near infrared.

Finally, Figure 5a corresponds to an intermediate case, associated with the ultraviolet bands. It can be observed that filtering in this range reduces the sample of 100,000 galaxies to one of 10,000. Due to the fact that for the analysis of populations at least one sufficiently energetic band was necessary (see section 1.2.1.), as an exception, the u band is included in the procedure.

As a consequence of SNR filtering and the imposed choice of bands, the final sample is reduced to 10,000 galaxies.

K correction

Once the signal-noise filter is applied for different color combinations, it is concluded that, despite obtaining a slight distinction compared to initial "raw" studies, the task of clearly discriminating the populations is still difficult.

In this way, the so-called K correction is then used, a type of correction applied to the magnitudes defined through equation (4) (Tavern, 2014). This new analysis arises

from the fact that the universe is expanding, a phenomenon that causes the entire spectrum of the galaxy to be shifted towards red. In this way, there is a difference between the flux (or apparent magnitude) emitted by the object from its reference system at rest and the value measured from the Earth's reference system.

By applying the K correction, it is therefore possible to estimate the “real” flux values of celestial bodies, providing much more reliable information (the K correction data used for each of the bands in the study sample have been obtained from ([Loveday, Norberg, & Baldry, February 2012](#))).

It is worth noting, however, that from the new sample of 10,000 galaxies from which we start, the sample is reduced to about 4,429 bodies in the end. This happens because: during the creation of the SNR filterThe condition had to be introduced that only those galaxies with K correction measurements were to be taken into account. This is consistent, since it would not make sense to work with signal-to-noise galaxies that did not then have an associated K correction measurement. Hence, by eliminating the data without this correction, the sample is reduced even further. However, the reason why there are no values for this parameter for some galaxies is unknown.

3. Result

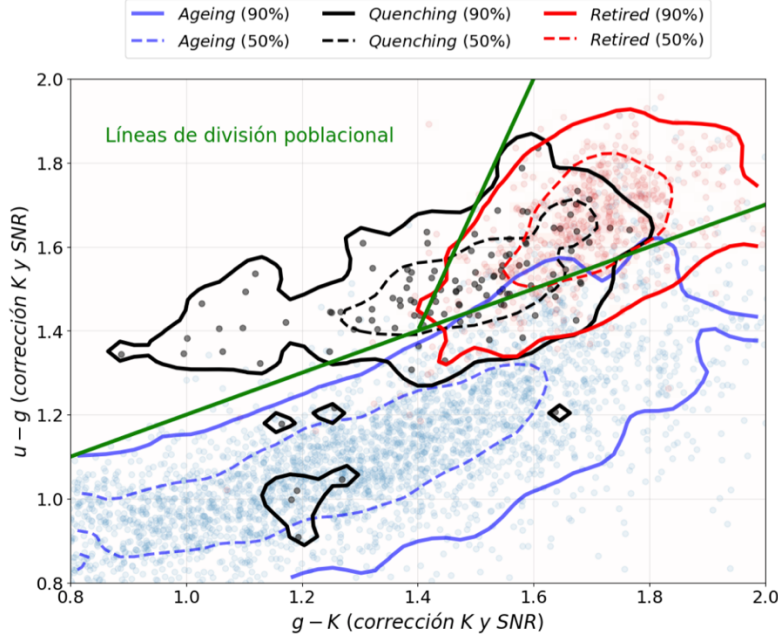
After studying several examples of color-color diagrams in detail, an important combination for the analysis was determined. It is the composition of magnitudes given by the following bands: $u - g$ versus $g - K$. This result was SNR filtered and K-corrected at the same time, obtaining the following representation (see figure 6).

This is a color-color diagram of 4,429 galaxies, represented by scattering populations of points: in blue the ageing (3,624 galaxies), quenching galaxies in black (118 galaxies) and finally retired galaxies in red (552 galaxies). The rest of the galaxies to complete the sample would be the undetermined ones that, as mentioned in section 2.1., remain unstudied during the project.

These three types of galaxies are delimited by smoothed contours that represent 90% (solid line) and 50% (dashed line) of the bulk of each population. In this way, it is possible to verify in the first instance the existence of two distinguishable sequences that

end in the retired region, the intersection point where the aged galaxies reside and with a very low SFR (negligible stellar activity) or zero (dead) (see section 2.1.).

Figure 6. Color-color diagram: $u - g$ versus $g - K$. Total representation of the sample with contours and population division lines. $g - K$

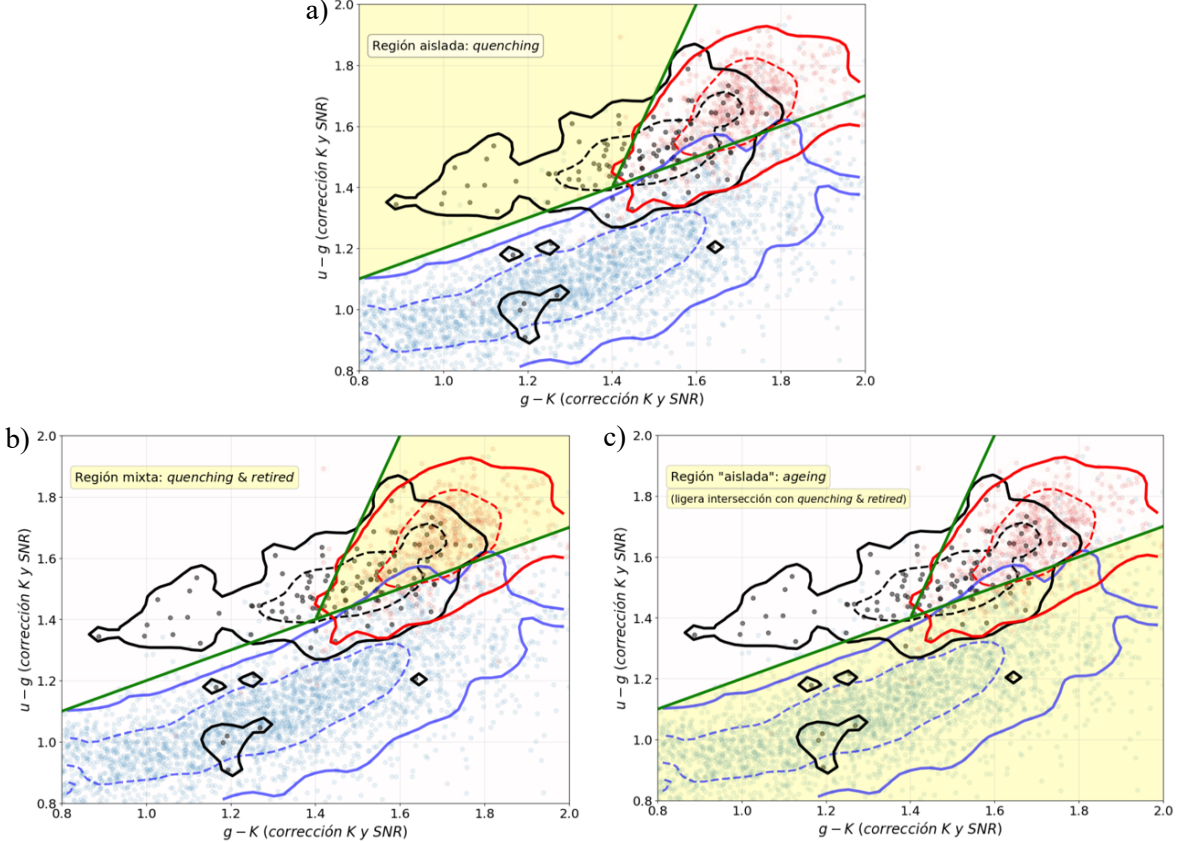


For galaxy classification, two demarcation lines are introduced, defined according to equation (9), which divide the map into three regions (see figures 6 and 7),

$$\begin{cases} (u - g) = 1,4 + \frac{(g - k) - 1,4}{2} \\ (u - g) = 1,4 + 2 \cdot ((g - k) - 1,4) \end{cases} \quad (9)$$

In this way, the feasibility of distinguishing populations by using photometric techniques and new separation lines is demonstrated. In this way, it is possible, first of all, to delimit the quenched galaxies from the rest (see figure 7a). Likewise, figure 7b includes the area of the diagram with contributions from quenching and retired populations. Finally, a region of ageing galaxies is recognized (figure 7c) in which some galaxies with a possible recent quenching process appear and a slight intersection with the previous mixed region.

Figure 7. Population classification. a) Isolated region of quenching galaxies. b) Mixed region of quenching and retired galaxies. c) “Isolated” region of ageing galaxies (with some recently quenching galaxies and intersection with retired galaxies).

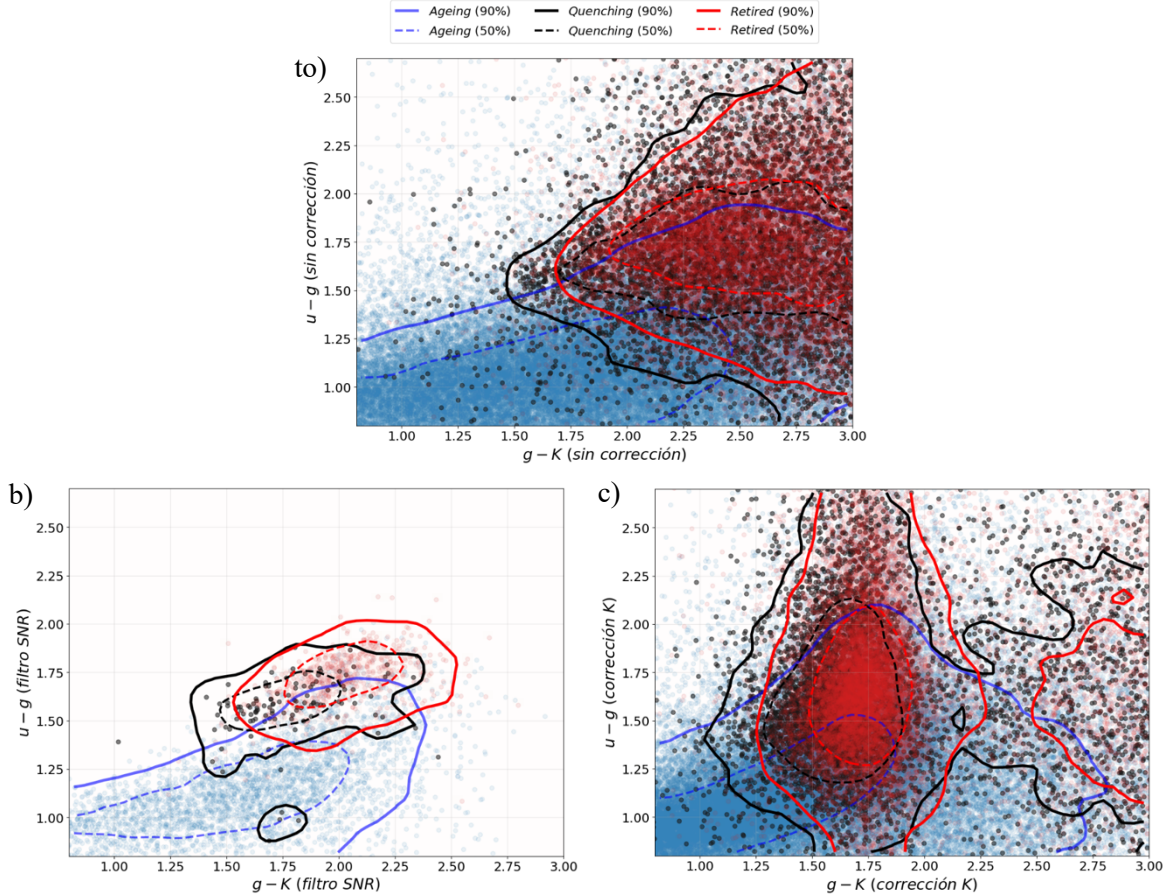


4. Discussion

As indicated in section 2.2.3., the process by which the final result of the project is reached consists of data manipulation through the use of different corrections. The reason why both K correction and *SNR* filtering had to be used at the same time is understood by observing figure 8.

Initially, the raw galaxy sample is represented, without any corrections (see figure 8a). In it, the need for data manipulation can be appreciated, since any attempt at classification is impossible due to the large amount of uncorrected information used, which only provides visual noise. As a consequence, it is impossible to delimit a double evolutionary sequence or a region where quenching galaxies predominate, which was the main objective.

Figure 8. Intermediate color-color diagrams (axis limits are modified for better visualization). a) Unmanipulated (raw) data. b) SNR-filtered data. c) K-corrected data.



Using only the signal-to-noise cutoff (see Figure 8b) then rapidly reduces the sample, allowing for a more noticeable distinction between the populations. A small region of the map where the quenching galaxies stand out becomes apparent. However, there is still a noticeable overlap between the quenching and retired populations, making a more precise delimitation impossible.

On the other hand, the consequences of imposing only K correction on the data are evaluated (see figure 8c). In this case, a modification of the position of the galaxies in the plane is observed, given the fact that the K correction shifts the spectrum of the galaxy to the left. Based on the type of initial spectrum of each galaxy, this shift would give new values for the color indices, causing a scattering of the populations to be observed and, again, preventing them from being differentiated. Thus, the conclusion remains the same as in the previous section.

These are the reasons why it was decided to use both corrections at the same time (see results in section 3), observing that when applied separately the desired result was not achieved, while together they constructed a map of corrected values with an adequate signal-to-noise ratio.

5. Conclusions

During the project, population classification is studied for a sample of 150,000 galaxies using photometric techniques as an alternative to spectroscopic results from previous studies.

Through color combinations, a successful diagram can be determined representing $u - g$ versus $g - K$. It verifies the distinction of two evolutionary sequences converging to the retired galaxy region as proposed in the AD. Also, a region of purely quenched galaxies is delimited, which satisfies the initial objective of the work. Likewise, two other extra areas are determined in the map: on the one hand, isolated ageing galaxies that end in a mixed region and that also have reduced groups of quenched galaxies (possibly due to having suffered a recent truncation episode); on the other hand, there is an intersection point of quenching and retired galaxies, verifying again the evolutionary paradigm of the AD.

On the one hand, it is important to highlight the importance of the choice of bands. As in spectroscopic parameterization, for photometry it is necessary to use colors with different time scales. Based on the results obtained, it is concluded that the colors $u - g$ and $g - K$ are a good choice: $u - g$ combines a near ultraviolet band (sensitive to the population of O and B stars) with a visible band (sensitive to all stars), while $g - K$ combines the visible band with a near infrared band (even more sensitive to the stellar population of type A and above). In this way there is an analogy between $u - g$ and $EW(H_{\alpha})$ (short time scales) and $g - K$ and $D(4000)$ (long time scales)

On the other hand, it is worth highlighting the possible existence of other successful band combinations for distinguishing populations. However, for the study it was not possible to determine them. With only 10 of the 21 available bands, only one result was determined using u, g y K . The main reasons why the signal-to-noise ratio for the

ultraviolet and mid-to-far infrared bands is so low are worth highlighting. Firstly, based on the blackbody approximation ([Black body, sf](#)) of the stars that make up galaxies, it is logical to observe that the radiation emitted by them in the ultraviolet is much lower than in the rest of the frequencies. This causes the quantity of ultraviolet photons that reach the telescopes to be lower, reducing the signal. For the infrared bands the opposite occurs. All bodies emit in this range, which causes the data obtained from the telescopes to have too much thermal noise, making it difficult to distinguish which of these photons come from the body of interest. Therefore, the SNR of the data is reduced again.

In conclusion, this type of photometric techniques is proposed as a first approximation of statistical analysis for the search for possible candidates for quenching galaxies. Once the different populations have been determined, a more exhaustive and detailed study could be carried out using spectroscopic procedures.

For future studies, knowing that the ultraviolet is a good tracer of the young stellar population, if telescopes could be built with more advanced technology and greater sensitivity in this band, the populations and their separation could be better characterized. Using better theoretical models for the K correction could also help to avoid losing data statistics during the analysis and to obtain more complete results.

References

- Noise, signal and SNR in amateur astrophotography.* (October 7, 2016). Obtained from Sideribus Astrophotography: <https://www.sideribus.com/blog/noise-snr-astrophotography-amateur>
- Equivalent width.* (sf). Retrieved from https://hmong.es/wiki/Equivalent_width
- Balmer Jump.* (June 8, 2021). Retrieved from Wikipedia, The Free Encyclopedia: https://en.wikipedia.org/wiki/Balmer_jump
- Galactic bulge.* (sf). Obtained from Wikipedia, The free encyclopedia: https://es.wikipedia.org/wiki/Bulbo_galáctico
- CALIFA: A panoramic view of the properties of galaxies.* (sf). Obtained from CALIFA SURVEY: <https://califa.caha.es>
- Asher. (September 8, 2011). One hundred years of the Hertzsprung-Russell diagram, the graph that organized the stars. Obtained from NAUKAS (science, skepticism and humor): <https://naukas.com/2011/09/08/cien-anos-del-diagrama-de-hertzsprung-russell-el-grafico-que-organizo-las-estrellas/>
- (2023). Spectroscopic data (information from private communication). (P. Corcho-Caballero, Editor)
- Corcho-Caballero, P., Ascasibar, Y., F. Sánchez, S., & López-Sánchez, Á. R. (13 January 2023). Ageing and Quenching through the ageing diagram: predictions from simulations and observational constraints. MNRAS.
- Corcho-Caballero, P., Casado, J., Ascasibar, Y., & García Benito, R. (29 July 2021). Galaxy evolution on resolved scales: ageing and quenching in CALIFA. MNRAS.

Cortese, L., Catinella, B., & Smith, R. (2021). The Dawes Review 9: The role of cold gas stripping on the star formation quenching of satellite galaxies. Cambridge University Press.

Black body. (sf). Obtained from Wikipedia, The free encyclopedia: https://es.wikipedia.org/wiki/Cuerpo_negro

Color-color diagram. (sf). Retrieved from https://hmong.es/wiki/Color-color_diagram

Saha ionization equilibrium equation. (sf). Retrieved from <http://astro.if.ufrgs.br/levato/leyeslte2/SAHA.htm>

Spectroscopy in Astronomy. (sf). Obtained from LibreTexts: [https://espanol.libretexts.org/Fisica/Astronom%C3%ADa_y_Cosmolog%C3%A1tica/Libro%C3%A1stico_Astronom%C3%ADa_\(OpenStax\)/05%C3%A1stico_Radiaci%C3%B3n_y_espectros/5.03%C3%A1stico_Espectroscopia_en_Astronom%C3%ADa](https://espanol.libretexts.org/Fisica/Astronom%C3%ADa_y_Cosmolog%C3%A1tica/Libro%C3%A1stico_Astronom%C3%ADa_(OpenStax)/05%C3%A1stico_Radiaci%C3%B3n_y_espectros/5.03%C3%A1stico_Espectroscopia_en_Astronom%C3%ADa)

F. López, M. (2019, August 26). Stellar Evolution: Main Sequence. Obtained from AstroAfición: <https://astroaficion.com/2019/08/26/evoluci%C3%B3n-estelar-secuencia-principal/>

Star formation. (sf). Obtained from Astronomy and Technological Developments, National Geographic Institute: <https://astronomia.ign.es/formacion-de-estrellas>

Photometry. (sf). Obtained from SEA: <https://www.sea-astronomia.es/glosario/fotometria>

Photometry. (sf). Obtained from Experimental Techniques in Astrophysics (Complutense University of Madrid): https://webs.um.es/bussons/tea_04_Fotometria.pdf

Galadí Enríquez, D. (2022, March 1). Fundamentals of astronomical photometry. Obtained from the Madrid Astronomical Association: <https://www.aam.org.es/fundamentos-de-fotometria-astronomica/>

Hydrogen-H. (sf). Obtained from LENNTECH:
<https://www.lenntech.es/periodica/elementos/h.htm>

Jansky (unit). (sf). Obtained from Wikipedia, The free encyclopedia:
[https://es.wikipedia.org/wiki/Jansky_\(unidad\)](https://es.wikipedia.org/wiki/Jansky_(unidad))

Kormendy, J., & Kennicutt Jr, RC (July 16, 2004). Secular Evolution and the Formation of Pseudobulges in Disk Galaxies. arxiv (Cornell University).

Spectroscopy in astronomy. (sf). Obtained from AstroMía:
<https://www.astromia.com/historia/espectrohistoria.htm>

Loveday, J., Norberg, P., & Baldry, IK (February 2012). Galaxy and Mass Assembly (GAMA): ugriz galaxy luminosity functions. ads (astrophysics data system).

Apparent magnitude. (sf). Obtained from Wikipedia, The free encyclopedia:
https://es.wikipedia.org/wiki/Magnitud_aparente

Sleeve. (sf). Obtained from SDSS: <https://www.sdss4.org/surveys/manga/>

Maragkoudaki, A., Zezas, A., Ashby, M.L., & Willner, S. (May 19, 2014). Aperture effects on spectroscopic galaxy activity classification. Monthly Notices of the Royal Astronomical Society.

Martínez Martínez, JL (January 9, 2018). The color of the stars and the spectrum. Obtained from Astronomy for all:
<https://astronomiaporatodos.com/2018/01/09/el-color-de-las-estrellas-y-el-espectro/>

Peng, Y., Maiolino, R., & Cochrane, R. (May 14, 2015). Strangulation as the primary mechanism for shutting down star formation in galaxies. Nature.

Project overview. (sf). Retrieved from Galaxy And Mass Assembly: <http://www.gama-survey.org>

Richer, M. (2022, September 13). Photometric systems. Retrieved from <http://www.astrosen.unam.mx/~richer/docencia/tecnicas/sistemafot.pdf>

Richmond, M. (n.d.). Astronomical "color". Retrieved from <http://spiff.rit.edu/classes/phys440/lectures/color/color.html>

Photometric system. (sf). Retrieved from https://hmong.es/wiki/Photometric_system

Taverna, M.A. (December 2014). Galaxy luminosity function from photometric redshifts. Retrieved from National University of Córdoba: [https://rdu.unc.edu.ar/bitstream/handle/11086/2785/TE%20A%20T_%20Taverna.pdf?sequence=1#:~:text=The%20K%2C%20K%20Correction%20\(z,rest%20system%20to%20z%20%3D%200](https://rdu.unc.edu.ar/bitstream/handle/11086/2785/TE%20A%20T_%20Taverna.pdf?sequence=1#:~:text=The%20K%2C%20K%20Correction%20(z,rest%20system%20to%20z%20%3D%200)

The IllustrisTNG project. (sf). Retrieved from <https://www.tng-project.org>

Wright, A.H., Robotham, A.S., & Bourne, N. e. (April 12, 2016). Galaxy And Mass Assembly: accurate panchromatic photometry from optical priors using LAMBDA.R. Monthly Notices of the Astronomical Society.